Study on Dynamic Prediction and Visualization Simulation of Fire Temperature Field Based on UAVs

Wenjiang Chen*, Jie Wang, Zhaoji Hu, Diping Yuan, Jinxing Hu and Jiaoyang Liu*

***Abstract*—In the process of petrochemical fire rescue, temperature is an important reference index, which can be used to analyze the possibility of domino accident and tank collapse. A method for predicting temperature field by bicubic spline interpolation is proposed in this paper. It collects data from unmanned aerial vehicles (UAVs), and the accuracy of prediction is influenced by the sampling strategy. It's not that the more UAV routes are, the higher the overall prediction accuracy of temperature field will be. And the smaller the data interval, the more conservative the prediction results in the high- temperature zones.**

***Index Terms*—cubic spline interpolation, unmanned aerial vehicles (UAVs), temperature field prediction, image similarity**

I. INTRODUCTION

The traditional method for fire spatial information acquisition is remote sensing, but there is a gap between it and emergency practice [1]. In recent years, with the investment of Chinese government in safety, unmanned aerial vehicles (UAVs) have become a kind of equipment. The flexibility and cheapness of UAVs are popular in the rescue of petrochemical fire [2]. UAV visualization can better help the safety inspection of the operation site [3]. In addition, UAVs are used for rescue in various accident scenes, such as fire control, monitoring, exploration, data collection, transmission of signals and so on [4, 5].

This paper will continue to study the application of UAV in petrochemical fire rescue. In case of fire, there are many uncertain factors [6]. Accurate and rapid prediction of temperature field can be used to prevent tank collapse or domino events [7] and protect the safety of firefighters [8], [9]. In this paper, a method is proposed to predict the temperature field of petrochemical fire by UAVs. The data acquisition process and prediction model of the UAVs are studied. By simulating a petrochemical fire process, the accuracy of the data acquisition strategy of the UAVs is analyzed. The application of this prediction method in engineering is studied theoretically.

Manuscript received May 24, 2022; revised June 6, 2022; accepted July 4, 2022, published March 17, 2023.

Wenjiang Chen and Diping Yuan are with Shenzhen Urban Public Safety and Technology Institute, Shenzhen 518046, China; Key Laboratory of Urban Safety Risk Monitoring and Early Warning, Ministry of Emergency Management, Shenzhen, Guangdong, 518038, China.

Wenjiang Chen and Jiaoyang Liu are with Changshu Institute of Technology, Suzhou 215500, China.

Wenjiang Chen and Jinxing Hu are with Shenzhen Institute of Advanced Technology, Chinese Academy of Sciences, Shenzhen 518055, China.

Jie Wang and Zhaoji Hu are with Nanchang University, Nanchang 330031, China.

*Correspondence: wjchen@cslg.edu.cn (W.C.); jyliu@cslg.edu.cn (J. L.)

II. DYNAMIC PREDICTION OF FIRE TEMPERATURE

A. The Method of Data Collection

Petrochemical fires are characterized by large scale and randomness, which can be destructive to equipment if rescue teams are not used in the correct way [10]. Fire exploration is the first step of fire rescue, which will be limited by terrain and environment. In the process of UAV investigation, it can realize all-round no dead angle investigation, which can not only improve the investigation efficiency, but also effectively improve the investigation effect [11]. With the development of UAV technology, UAVs are playing an increasingly important role in fire exploration [12].

The data of the temperature field in a fire are collected by UAVs for the dynamic prediction. The hardware system of UAV includes UAV body, Global Positioning System (GPS) module, tripod head, wireless transmission module, temperature sensor and camera. As shown in Fig. 1, the communication protocol between UAVs and ground station is micro air vehicle link (MAV Link) [13]. And the communication protocol of GPS is NMEA-0183 [14]. In order to reduce the difficulty of operation, leader-follower structure is designed in UAV formation. Communication links in communication network topology are used to realize information exchange during UAV formation flight. As shown in Fig. 2, the operator controls the speed, height, spacing, coordinates and direction of the leader. Followers receive the leader's flight information and interval instructions to confirm their formation requirements. And they only transmit image information, temperature data, and location information to ground stations. Unless the leader fails, a follower can be selected as the new leader to receive instructions from the ground station.

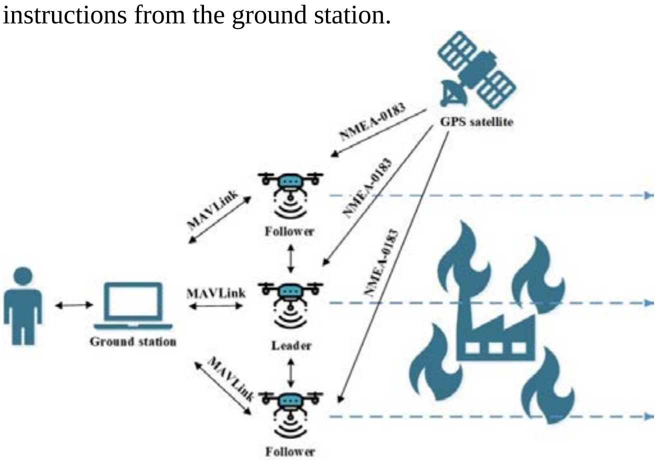

Fig. 1. Communication process diagram.

DOI: 10.7763/IJMO.2023.V13.821

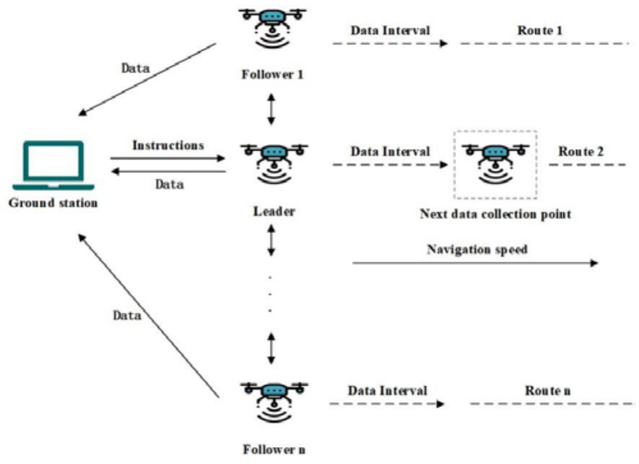

Fig. 2. The method of data collection.

The data interval is affected by the navigation speed of the UAV, which can be controlled by the operator. The product of the UAV's navigation speed and the sensor's sampling period is the data interval. Therefore, the navigation speed of UAVs indirectly affects the accuracy of dynamic prediction. The influence of data interval on the accuracy of dynamic prediction will be studied in the discussion.

B. The Data Analysis Prediction

Comparing the different spline interpolation method on the greenhouse temperature field visualization performance in reference [15], the result is that the bicubic spline interpolation method is applicable to the temperature field fitting at a certain moment. Cubic spline interpolation is a method of constructing cubic functions from known data and approaching the minimum points of functions to be solved with their minimum points [16]. The temperature in its output picture changes smoothly by UAV camera. and has a temperature gradient, which can be a good guide for the rescue teams.

Because the final result is the three-dimensional relationship between temperature and horizontal coordinates, bicubic spline interpolation method is used to obtain the relationship [17]. And the method is used to fit the prediction image composed of collected data [18]. Construct a two-dimensional relative coordinate system with the ground station as the origin point. Coordinate X in the same direction of travel on the plane of UAVs. Coordinate Y perpendicular to the direction of travel on the plane of UAVs. Every UAV delivers three parameters to the ground station for prediction. They are the coordinates $(x_{i,j}, y_{i,j})$ and temperature $T_{i,j}$ for each data collection point.

Bicubic spline interpolation first divides the whole large interval into multiple cells. There are $(m+1)\times(n+1)$ data points in the space S_0, which is divided into $m\times n$ small spaces $S_{i,j}$

$$S_{i,j} = [x_{i-1}, x_i] \otimes [y_{j-1}, y_j], i = 0,1,...m; j = 0,1,...,n \quad (1)$$

$$S_{i,j} \in S_0 \{(x, y) \mid a = x_0 \le x \le x_{m+1} = b \cap c = y_0 \le y \le y_{n+1} = d\} \quad (2)$$

The temperature function is defined as:

$$P = (x_{i,j}, y_{i,j}, T_{i,j}), i = 0,1,..., m; j = 0,1,..., n \quad (3)$$

Eq. (4) is that in each small cell, the temperature T is cubic polynomial. And the partial derivative of each node in adjacent cell is continuous.

$$T(x, y) = \sum_{k=0}^{3} \sum_{l=0}^{3} A_{i,j,k,l} \left(\frac{x - x_{i-1}}{x_i - x_{i-1}}\right)^k \left(\frac{y - y_{j-1}}{y_j - y_{j-1}}\right)^l, \quad (4)$$
$$i = 0,1,..., m; j = 0,1,..., n$$

Eq. (4) shows that there are $(m+3)\times(n+3)$ undetermined coefficients $\{A_{i,j,k,l}\}$ in its expression. But only $(m+1)\times(n+1)$ data points are known, leaving $2(m+1)+2(n+1)+4$ remaining degrees of freedom. Therefore, the range that can be predicted by using $(m+1)\times(n+1)$ data points is $(m-1)\times(n-1)$.

III. Fire Simulation and Analysis

A. Simulation Introduction

This work shows how to simulate a pool fire development by a tank storing liquefied petroleum gas (LPG). The simulation is used in two aspects of follow-up research: provide data and data comparison.

The software used for the simulation is PYROSIM 2019 developed by Thunderhead Engineering, which is mostly used for fire simulation. It can accurately predict and analyze the temperature, movement and concentration of fire and flue gas.

B. Geometric Model and Boundary Conditions

There are 6 groups of tanks storing liquefied petroleum gas, 4 tanks with a volume of 5000 m^3 in each of 4 groups, and 6 tanks with a volume of 5000 m^3 in each of 2 groups, shown in Fig. 3. Furthermore, fire dikes are set up for each group of containers. The model does not consider the effect of tank fire sprinklers on fire temperature.

In order to reduce the amount of calculation, the real model is reduced by a ratio of 1:10. The model of the tank is 1.5 m high and 2.4 m diameter. The height of the fire dikes model is 0.25 m. The ambient temperature is 25 ℃. The wind speed of the model is 1.0 m/s. Excluding the ground and the direction of the wind, the other directions are opened.

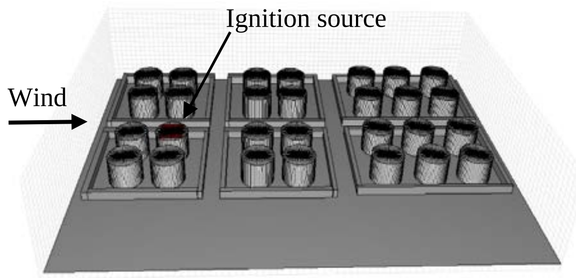

Fig. 3. Three-dimensional model of fire simulation.

C. Simulation Results

Since wind field loading takes some time, the fire burns in a windless environment within 0 to 10s, during which time the flame shape is similar to a straight cylinder, as shown in

Fig. 4(a). As shown in Fig. 4(b), within 10 to 60s, the flame evolves from a straight cylinder into an oblique cylinder. As shown in Fig. 4(b) and Fig. 4(c), the flame reaches its maximum tilt angle at a certain point in time, and the shape of the flame remains the same, but the smoke will spread with the wind. As shown in Fig. 4(d), after 60s, the fire site has reached a stable state. The circulating state of flue gas makes it easier for flue gas to diffuse in the form of surface between tank groups [19].

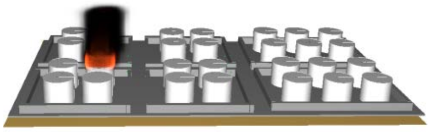

(a). Fire simulation in the windless

(b). Fire propagation under wind speed loading

(c). Flue gas stability under wind speed loading

(d). Flame stability under wind speed loading

Fig. 4. 3D visualization of fire development.

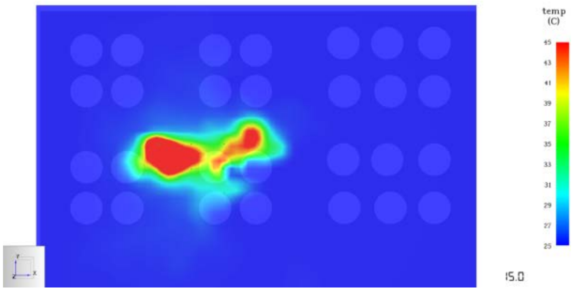

(a). 15s, the fire plane temperature distribution

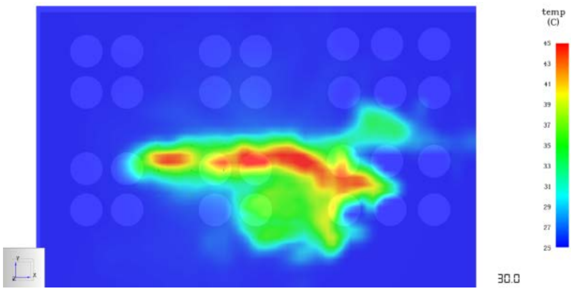

(b). 30s, the fire plane temperature distribution

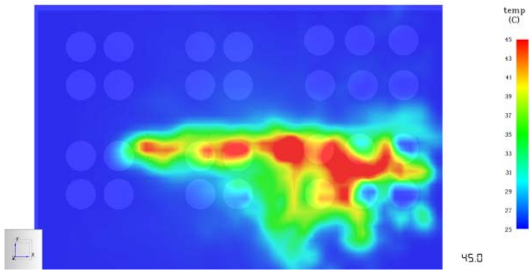

(c). 45s, the fire plane temperature distribution

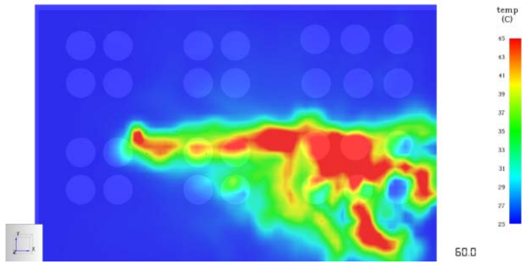

(d). 60s, the fire plane temperature distribution

Fig. 5. Development of fire plane temperature distribution.

Fig. 5 shows the temperature development process over time on the fire plane, thermal feedback on blockages is enhanced by blockages nearby pool fires, which is consistent with the conclusion in reference [20].

IV. Visualization of Fire Temperature Field

A. *Visual Introduction*

This work will simulate the process of temperature data collection of UAVs. On the fire simulation model, thermocouples are arranged on the data acquisition path of the UAVs to collect the data. The temperature field predicted by the data will be compared with the simulated image results. This will be used to compare the accuracy of predictions of different temperature gradients at different times. Actually, the temperature changes with time and therefore does with the data collection time. In this paper, lose sight of the change, and hypothesis: The UAV's data collection process does not take time.

B. *Temperature Data Based on UAV*

Simulation scenarios for 30th and 45th seconds are used as the predictors of the temperature field, as shown in Table I and Table II. Set up five UAV routes with a data interval of 4 m and set 9 thermocouples on each route. The route parameter of UAV route (1) is $y_1 = 15$ m and $z_1 = 1.5$ m; the route parameter of UAV route (2) is $y_2 = 11$ m and $z_2 = 1.5$ m; the route parameter of UAV route (3) is $y_3 = 7$ m and $z_3 = 1.5$ m; the route parameter of UAV route (4) is $y_4 = 3$m and $z_4 = 1.5$ m; the route parameter of UAV route (5) is $y_5 = -1$ m and $z_5 = 1.5$ m.

TABLE I: The Temperature Data for the 30th Second

T (℃), z = 1.5 m									
x_i / y_i	14 m	18 m	22 m	26 m	30 m	34 m	38 m	42 m	46 m
15 m	25.75	26.3	25.95	26.41	25.96	25.78	26.90	34.51	25.17
11 m	48.89	44.63	45.25	46.01	47.47	40.11	26.84	25.28	25.09
7 m	26.75	29.63	29.74	33.08	35.10	40.88	43.63	35.90	25.00
3 m	25.40	25.95	26.42	32.39	36.19	41.00	25.10	25.02	25.00

-1 m	25.41	25.59	25.62	26.02	27.78	27.82	25.03	25.01	25.00

TABLE II: THE TEMPERATURE DATA FOR THE 45TH SECOND

T (℃), z = 1.5 m

x_i \ y_i	14 m	18 m	22 m	26 m	30 m	34 m	38 m	42 m	46m
15 m	25.61	26.12	25.94	27.14	27.50	26.11	25.92	26.94	27.59
11 m	50.96	43.99	43.19	45.82	46.43	56.23	44.04	28.78	29.39
7 m	26.62	29.78	29.42	32.38	33.64	43.66	41.58	46.93	34.3
3 m	25.33	25.81	26.60	27.22	32.55	40.49	44.35	32.80	25.34
-1 m	25.31	25.47	25.69	25.81	29.35	29.80	25.51	36.83	25.09

C. Predictive Image of the Temperature Field

Bicubic spline interpolation of temperature data is the core of dynamic prediction. Fig. 6 shows a visualization of the cube interpolation of temperature data. The predicted temperature line changes gently and the temperature changes in a gradient.

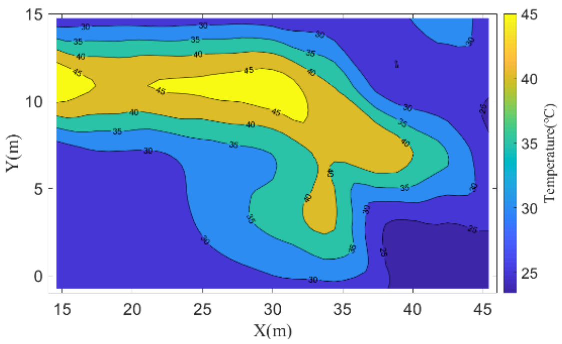

(a). Fire temperature map of the 30th second

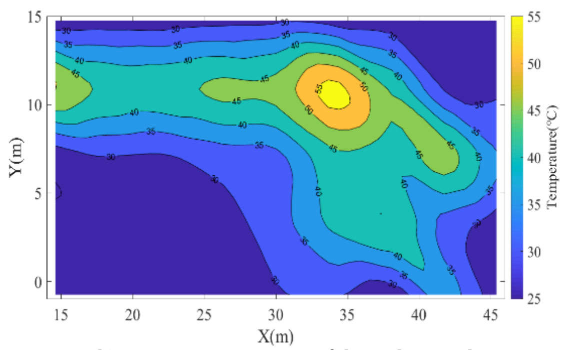

(b). Fire temperature map of the 45th second

Fig. 6. The temperature distribution map based on bicubic spline interpolation.

The high-temperature area of fire is an important parameter in the dynamic prediction results of the temperature field. Fig. 7 and Fig. 8 show predictive and simulated images at different temperatures in the same area.

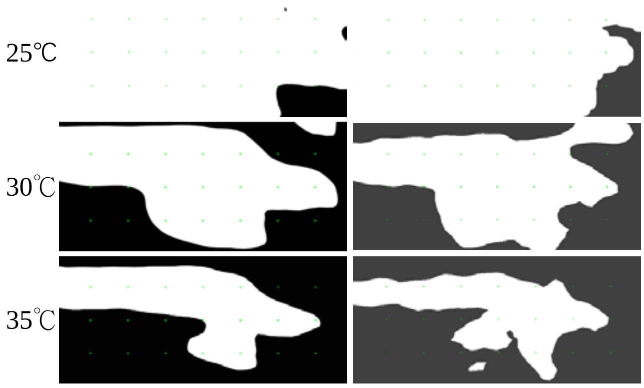

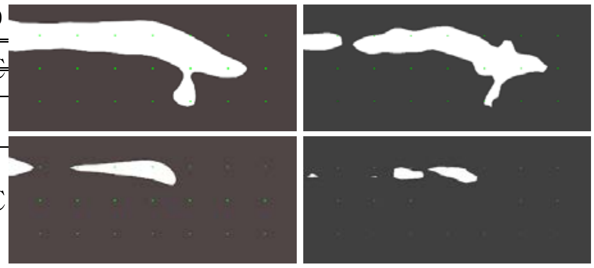

Fig. 7. Comparison of bicubic spline interpolated image (left) and simulated image (right) at different temperatures in the 30th second.

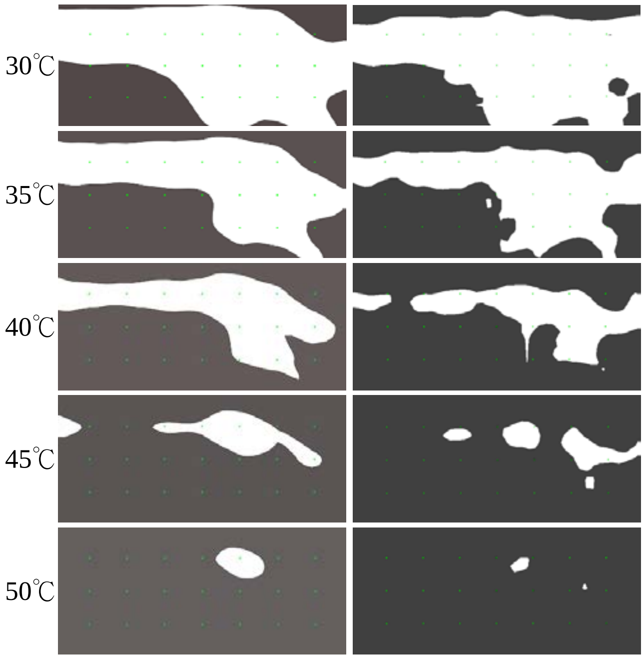

Fig. 8. Comparison of bicubic spline interpolated image (left) and simulated image (right) at different temperatures in the 45th second.

D. Image Similarity Comparison and Analysis

In engineering applications, a visual image of the fire temperature field has been calculated before. This work is to verify the similarity between the predicted image and the simulated image, which is in place of real fire conditions. This image similarity comparison is based on the perceptual hash algorithm (PHA) [21]. As shown in Fig. 9, the basic principle is to convert the image feature into a "fingerprint" string, and to compare the "fingerprint" to get the similarity of the image. The steps of the perceived hash algorithm are as follows:

Step 1: Read the picture data and reduce the picture for grayscale processing, into 256 orders of grayscale map.

Step 2: Reduce it to 32 × 32 sizes.

Step 3: Calculate the discrete cosine transformation (DCT). The DCT of the grayscale graph is carried out by the frequency and trapezoidal decomposition for the picture, and the DCT matrix of 32 × 32 is obtained.

Step 4: Zoom out of the DCT matrix. In the DCT results obtained by step 3, the 8 × 8 matrix in the upper left corner is retained, representing the lowest frequency of the picture.

Step 5: Calculate and reduce the average of the DCT matrix, traversal the matrix, and get the hash fingerprint map of 8 × 8.

Step 6: Calculate the similarity using the Hamming distance.

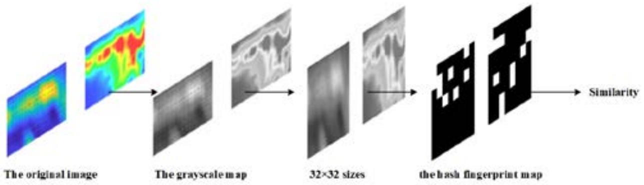

Fig. 9. The process of image similarity comparison.

Fig. 10 shows the similarity between the bicubic spline interpolated image and simulated image in Fig. 7 and Fig. 8. The higher the similarity, the greater the accuracy of the prediction. As can be seen from Fig. 9, under this method of prediction of temperature field, the prediction accuracy of different temperature regions is close.

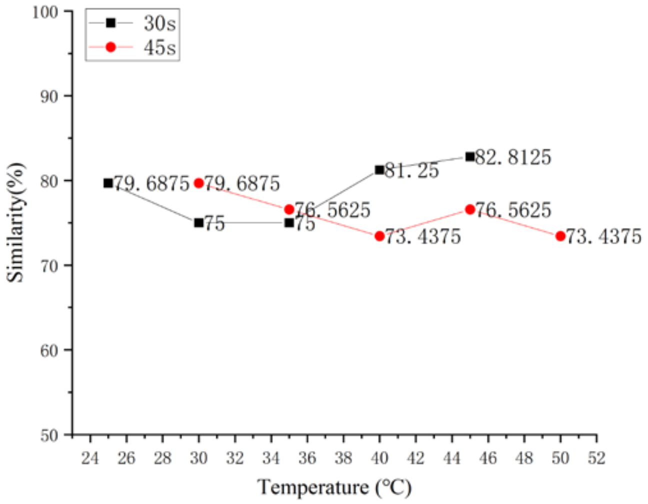

Fig. 10. The similarity curve between the bicubic spline interpolated image and the simulated image.

The comparison of image similarity is a conservative method. During the comparison of image similarity, the area that does not actually occur but is predicted to occur is a conservative prediction area. The prediction result of this area will make the rescue team take too much rescue and will not affect the rescue team to take wrong measures. As shown in Fig. 8, there are many conservative prediction areas, so the image similarity data obtained in Fig. 10 will be lower than the prediction results actually used for fire rescue.

V. Discussion

In the analysis of fire simulation and visualization results, we have investigated the similarity of visual images obtained by bicubic spline interpolation method. The results show that the similarity between the temperature field image and the simulated image obtained by this method is more than 70%. The amount of data has an important effect on the accuracy of the visual image. Therefore, we investigated the effect of data volume on the accuracy of visual images, the technical route chosen is the same as before, and the solution process is omitted here.

From the data acquisition process, it can be concluded that there are two factors that determine the amount of data: the number of UAV routes ΔR and the data interval ΔL. Therefore, we changed the number of UAV routes and the data interval separately, based on previously investigated models. We considered the UAV routes ΔR = {4, 5 ,6, 7, 8}, with a data interval ΔL = 4 m and the UAV routes ΔR = 5, with data intervals ΔL = {5 m, 4.5 m, 4 m, 3.5 m, 3 m, 2.5 m}. As Shown in Fig. 11, these images are grayscale and reduced to 32 × 32 sizes.

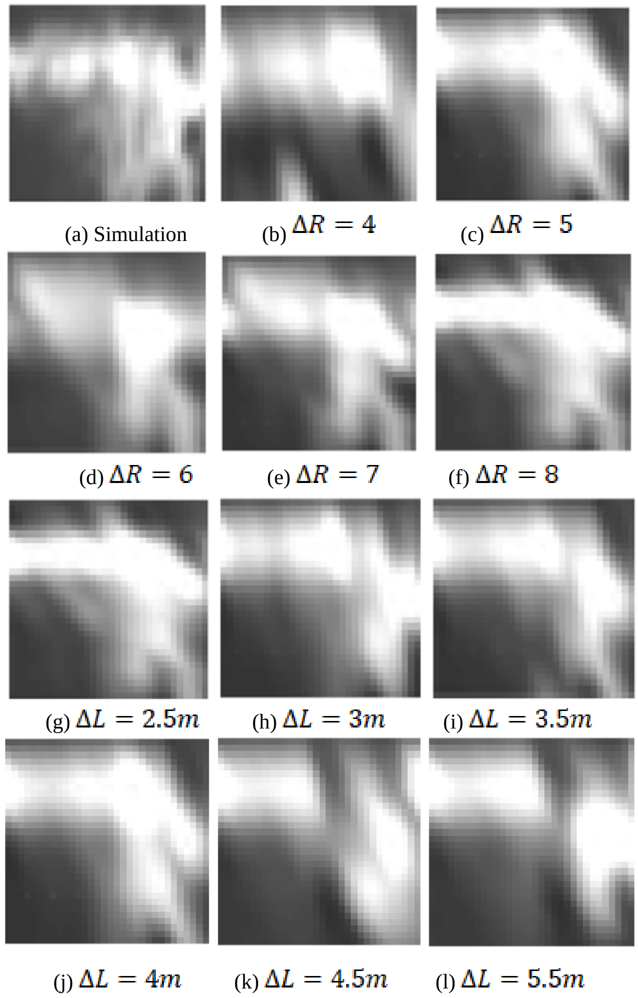

Fig. 11. Predictive images under different data acquisition strategies.

We compared the similarity between the predicted image and the simulated image. The similarity results are shown in Fig. 12. The number of routes has a greater impact on image accuracy, but the cost of the application will increase. And the data interval will affect the calculator's calculation time. Theoretically, there must be a deviation in the predicted result. But the benefit of this method is that it provides quantifiable field data for rescue teams. These data can be used to conduct in-depth studies of fire temperature fields.

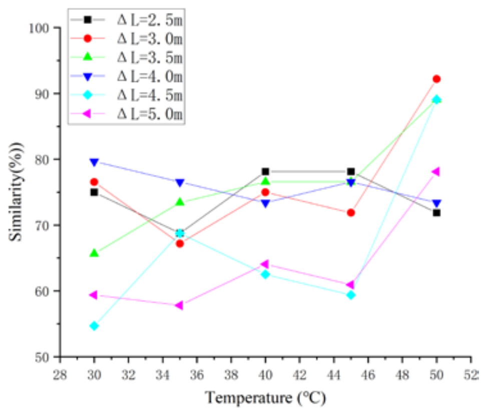

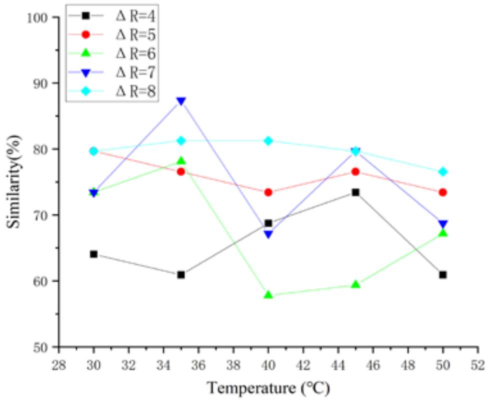

Fig. 12. Predicted image similarity for different quantity routes and different data intervals.

Image similarity is one of the fastest evaluation methods. Most of the similarity in Fig. 12 is between 60% and 80%. This comparison result is relatively low. From the principle of image similarity, the size of the image range will affect the similarity result. Therefore, we don't have to pay too much attention to the value of similarity, we pay more attention to the rules of strategies that can improve the similarity. We compared the quantitative results of Fig. 12 with the qualitative results of Fig. 10. Obviously, it's not that the more UAV routes there are, the smoother the predictions are for different temperature ranges. The data interval has a greater effect on the prediction accuracy of the high-temperature zones than in the low-temperature zones. Conclusively, the most appropriate number of routes is $\Delta R = \{5, 8\}$ and the most appropriate data intervals is 2.5–4 m. We hope these findings can help to operate UAVs on site.

VI. Conclusion

In this paper, a method for predicting temperature field of petrochemical fire using UAVs to collect field data is proposed. The process of simulating petrochemical fires is used to theoretically verify the accuracy of the prediction method. The results are as follows:

(1) In the simulation of this paper, the similarity of the predicted image of double three spline interpolation is 60% to 85%. Because the accuracy of the prediction is influenced by the drone's sampling strategy, it is possible to be higher than 85%. Sampling strategy mainly includes data interval and route number.

(2) The speed of the UAV and the sampling cycle of the sensor determine the data interval. The data interval has a greater effect on the prediction results of the fire high-temperature zones. The smaller the data interval, the wider the range of conservative predictions for high temperature zones.

(3) The overall prediction accuracy is more affected by the number of UAV routes. It's not that the more UAV routes there are, the more accurate and stable the overall prediction will be.

Conflict of Interest

The authors declared that they have no conflicts of interest to this work. We declare that we do not have any commercial or associative interest that represents a conflict of interest in connection with the work submitted.

Author Contributions

Wenjiang Chen, Diping Yuan, Jinxing Hu contributed to the conception of the study; Jie Wang, Jiaoyang Liu performed the simulation experiment; Jie Wang, Zhaoji Hu performed the data analyses and wrote the manuscript; all authors had approved the final version.

Funding

This work was supported by Supported by Shenzhen Urban Public Safety and Technology Institute, and Key Laboratory of Urban Safety Risk Monitoring and Early Warning, Ministry of Emergency Management, and Shenzhen Science and Technology Program (ZDSYS20210929115800001).

References

[1] X. Zheng, F. Wang, M. Qi, Q. Meng, "Planning remote sensing emergency services: Bridging the gap between remote sensing science and emergency practice in China," *Safety Science*, vol. 141, September 2021.

[2] S. Ding, J. Chen, H. Hu, *et al*., "Application and Research of Uav in Petrochemical Fire," Guangdong chemical industry, vol. 47, no. 11, pp. 121–122, 2020.

[3] R. R. S. d. Melo, D. B. Costa, J. S. Álvares, and J. Irizarry, "Applicability of unmanned aerial system (UAS) for safety inspection on construction sites," *Safety Science*, vol. 98, pp. 174–185, 2017.

[4] M. Gheisari, and B. Esmaeili, "Applications and requirements of unmanned aerial systems (UASs) for construction safety," *Safety Science*, vol. 118, pp. 230–240, 2019.

[5] I. Jeelani, and M. Gheisari, "Safety challenges of UAV integration in construction: Conceptual analysis and future research roadmap," *Safety Science*, vol. 144, 2021.

[6] Z. Wang, K. Lu, L. Feng, *et al.*, "Simulation on smoke re-circulation transition in an urban street canyon for different fire source locations with cross wind," *Safety Science*, vol. 127, 2020.

[7] M. Zhang, F. Zheng, F. Chen, W. Pan, and S. Mo, "Propagation probability of domino effect based on analysis of accident chain in storage tank area," *Journal of Loss Prevention in the Process Industries*, vol. 62, 2019.

[8] G.P. Horn, J.W. Stewart, R.M. Kesler, *et al.*, "Firefighter and fire instructor's physiological responses and safety in various training fire environments," *Safety Science*, vol. 116, pp. 287–294, 2019.

[9] G. Zhang, S Yan, G. Zhu, P. Feng, and B. Jia, "Smart firefighting construction in China: Status, problems, and reflections," *Fire and Materials*, vol. 44, no. 4, pp. 479–486, 2020.

[10] L. Ding, J. Ji, F. Khan, "Combining uncertainty reasoning and deterministic modeling for risk analysis of fire-induced domino effects," *Safety Science*, vol. 129, 2020.

[11] B. Wang, D. Li, C Wu, "Characteristics of hazardous chemical accidents during hot season in China from 1989 to 2019: A statistical investigation," *Safety Science*, vol. 129, 2020.

[12] Y. Zeng, Q. Duan, X. Chen, D. Peng, Y. Mao, and K. Yang, "UAVData: A dataset for unmanned aerial vehicle detection," *Soft Computing*, vol. 25, pp. 5385–5393, 2021.

[13] N. Demiannay, N. Besnier, C. Thomas, V. Thapa, V. Devalla, and A. K. Mondal, "Design and Development of Multirotor UAV with Automatic Collision Avoidance using Stereo Camera," *INCAS BULLETIN*, vol. 12, no. 3, pp. 65-75, September 2020.

[14] S. G. Volosov, S. A. Korolyov, V. N. Nestyorkin, S. A. Tarasov, "Methods and Means of Synchronizing Seismic Stations Operating under Conditions of Inaccessibility of GPS Satellite Signals," *Seismic Instruments*, vol. 57, pp. 397–408, 2021.

[15] X. Xiao, M. Cheng, H. Yuan, *et al.*, "Visual simulation analysis of green house temperature field based on interpolation method," *Journal of Chinese Agricultural Mechanization*, vol. 42, no. 1, pp. 75–84, 2021.

[16] X. Wang, Y. Wang, Z. Cao, *et al.*, "Comparison Study on Linear Interpolation and Cubic B-Spline Interpolation Proper Orthogonal Decomposition Methods," *Advances in Mechanical Engineering*, vol. 5, 2013.
[17] X. Han, and J. Han, "Bicubic B-spline surfaces constrained by the Biharmonic PDE," *Applied Mathematics and Computation*, vol. 361, no. 15, pp. 766-776, 2019.
[18] J. Noor, S. I. Salim, and A. B. M. A. Islam, "Strategizing secured image storing and efficient image retrieval through a new cloud framework," *Journal of Network and Computer Applications*, vol. 192, 2021.
[19] L. Wang, and D. Rajan. "An image similarity descriptor for classification tasks," *Journal of Visual Communication and Image Representation*, vol. 71, 2020.
[20] J. Han, P. Geng, Z. Wang, F. Wang, M. Weng, and F. Liu, "Effects of fire-blockage distance on pool fire burning behavior and thermal temperature profiles in a naturally ventilated tunnel," *Tunnelling and Underground Space Technology*, vol. 117, 2021.
[21] K. Ding, Z. Yang, Y. Wang, and Y. Liu, "An Improved Perceptual Hash Algorithm Based on U-Net for the Authentication of High-Resolution Remote Sensing Image," *Applied Sciences*, vol. 9, no. 15, p. 2972, July 2019.

Wenjiang Chen is a postdoctoral researcher at Shenzhen Institutes of Advanced Technology, Chinese Academy of Sciences. Currently, he works at Shenzhen Urban Public Safety and Technology Institute, Changshu Institute of Technology as the chief chair of department. He has granted his PhD in solid mechanics from Nanchang University in 2019. He studied at Florida Atlantic University, USA as a visiting scholar from 2017 to 2018. His thesis explored accident mechanism and application of computer technology in accident simulation. His research interests are information technologies in urban public safety, system safety and risk analysis.

Jie Wang received the B. Eng. Degree in process equipment and control engineering from Nanchang University, China in 2019. He is pursuing the M. S. degree in power engineering from Nanchang University, China. Currently, he works at Shenzhen Urban Public Safety and Technology Institute as a research assistant. His research interests are information technologies in urban public safety, system safety and risk analysis.

Zhaoji Hu is currently a professor with Nanchang University, China. His research interests include development of new process equipment, failure analysis and accident prevention of process equipment, and information technology of process equipment . He received a Ph.D. degree in chemical process machinery from East China University of Science and Technology, China, in 1998. Between 2006-2007, he was a visiting scholar at University of Nottingham, UK.

Diping Yuan works at Shenzhen Urban Public Safety and Technology Institute as the chief technology officer, Shenzhen Institute in China University of Mining and Technology as the chief officer. He is with Shenzhen Institutes of Advanced Technology, Chinese Academy of Sciences as a professor, doctoral supervisor and the chief scientist of smart emergency. His research interests are fire fighting and rescue technology, smart emergency and information technologies in urban public safety.

Jinxing Hu works at Shenzhen Institutes of Advanced Technology, Chinese Academy of Sciences as a professor, doctoral supervisor and the director of smart city research office. He has granted his PhD in spatial information technology from Peking University. He worked at Shanghai Jiaotong University as a postdoctoral researcher. He has participated in many research projects on geographic information system, artificial intelligence and big data. His research interests are geographic spatial intelligence, big data and smart emergency.

Jiaoyang Liu works at Changshu Institute of Technology. She received the B. Eng. Degree in process equipment and control engineering from Zhengzhou University, China in 2007, and M. S. degree in chemical process machinery from South China University of Technology, China in 2010, respectively. Her research interests are enhanced heat transfer, chemical equipment safety, information technologies in urban public safety, system safety and risk analysis.